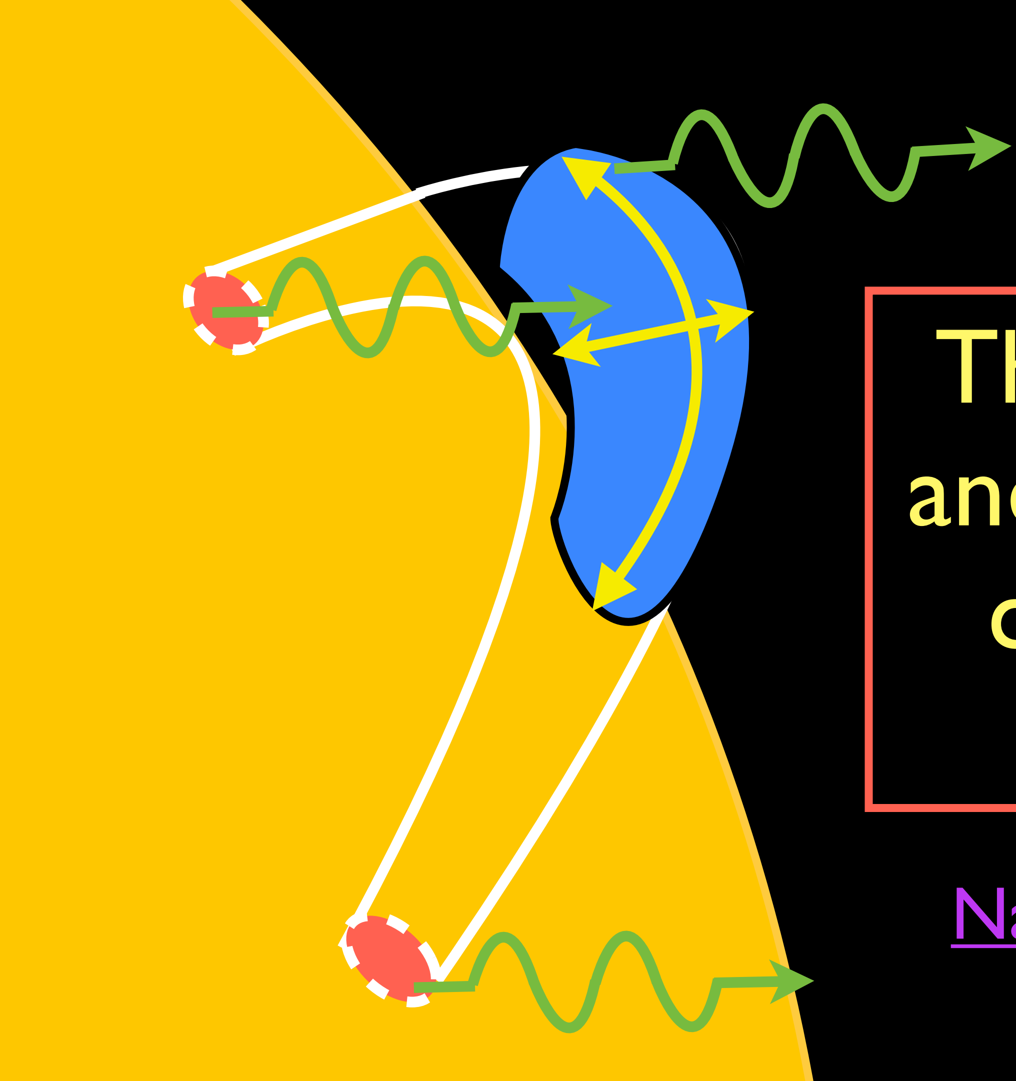

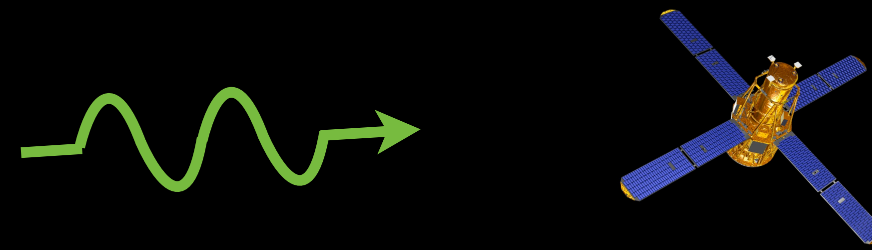

The time evolving spatial and spectral properties of coronal X-ray sources from solar flares.

Natasha Jeffrey and Eduard Kontar
University of Glasgow

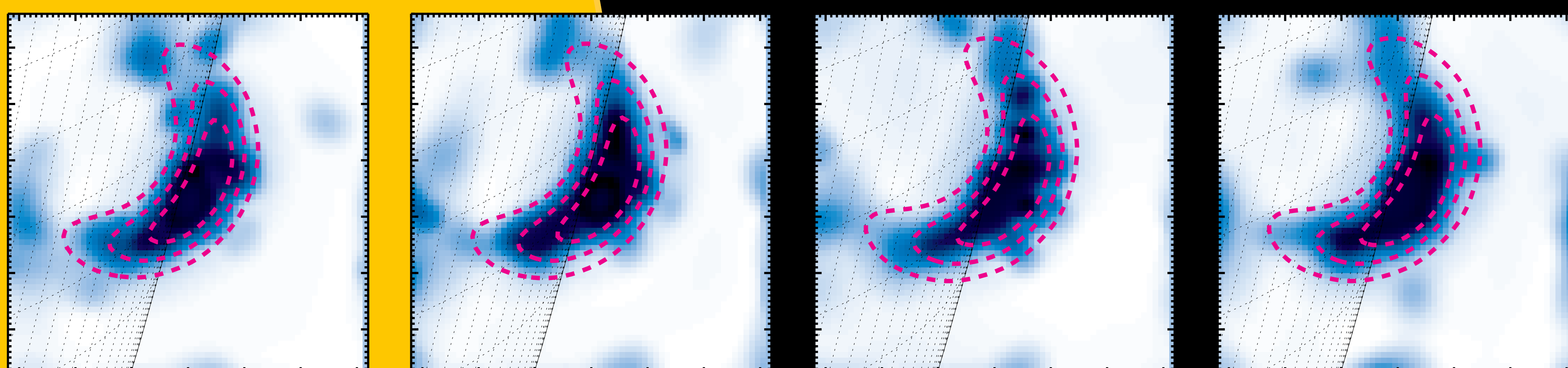

Solar flare X-ray coronal sources

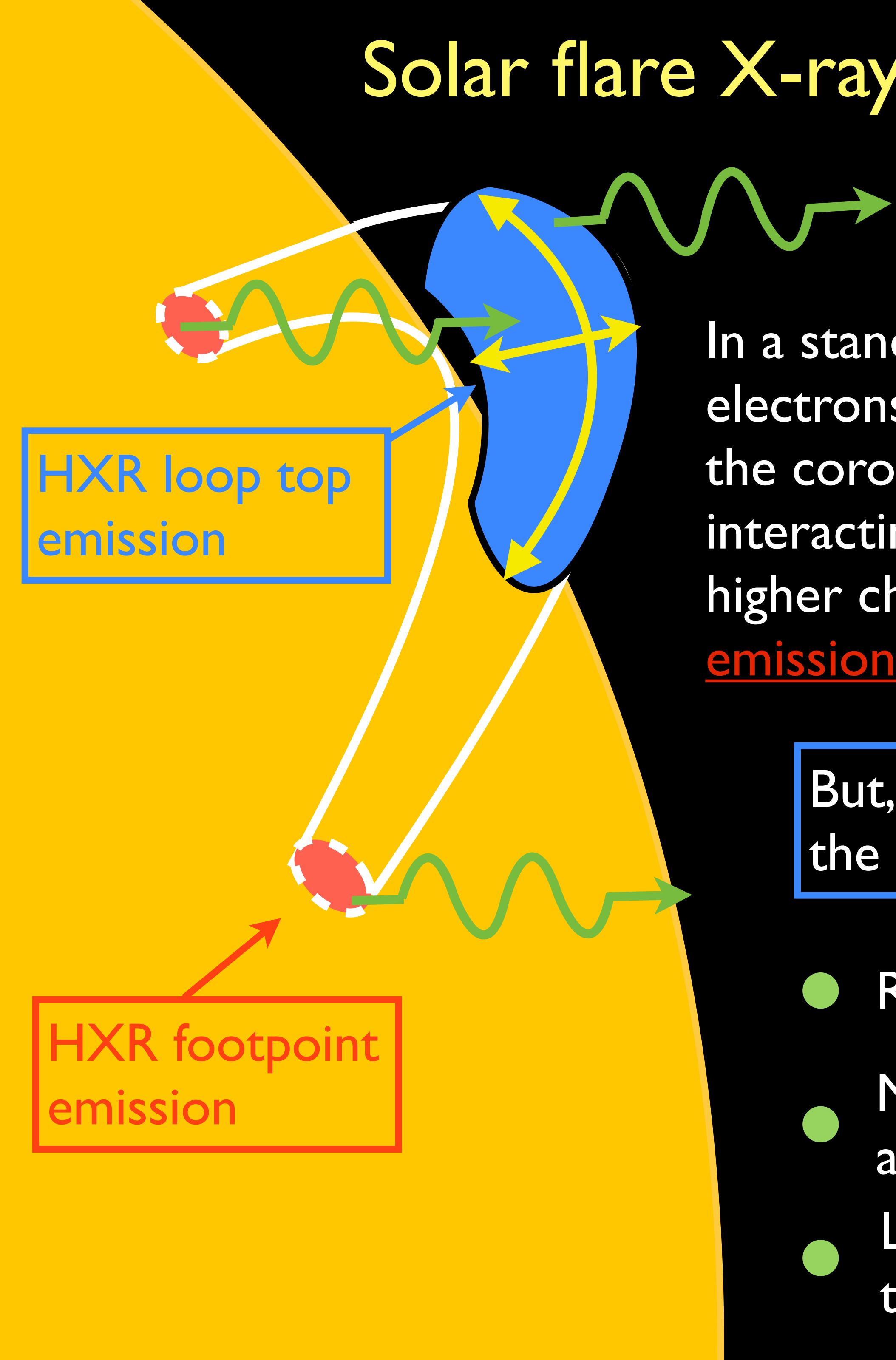

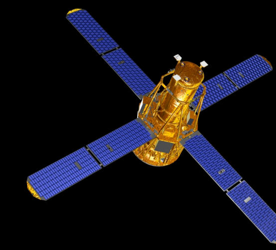

In a standard flare model, generally think of electrons being accelerated by some process in the corona and travelling along field lines before interacting via HXR bremsstrahlung in the higher chromospheric densities - footpoint emission.

But, we also see X-ray emission from the corona - loop top emission.

- Regions of high coronal density.
- Much closer to the site of initial particle acceleration.
- Loop top observations - help constrain transport/acceleration models.

Finding suitable coronal events

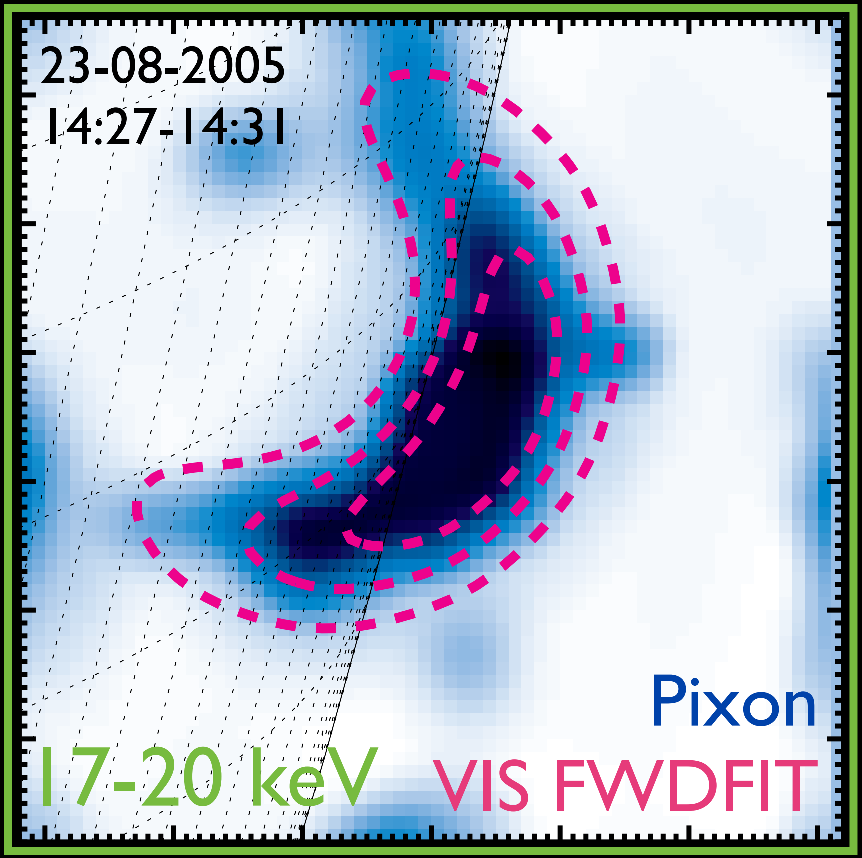

- Each of our chosen events were previously studied by Xu et al. (2008) and Kontar et al. (2011) - i.e. see Iain's talk.
- All three events are similar M-class flares.
- Using different imaging algorithms (Clean and Pixon), each source appears as a loop-like structure that can be fitted with a VIS FWDFIT loop.

Finding suitable coronal events

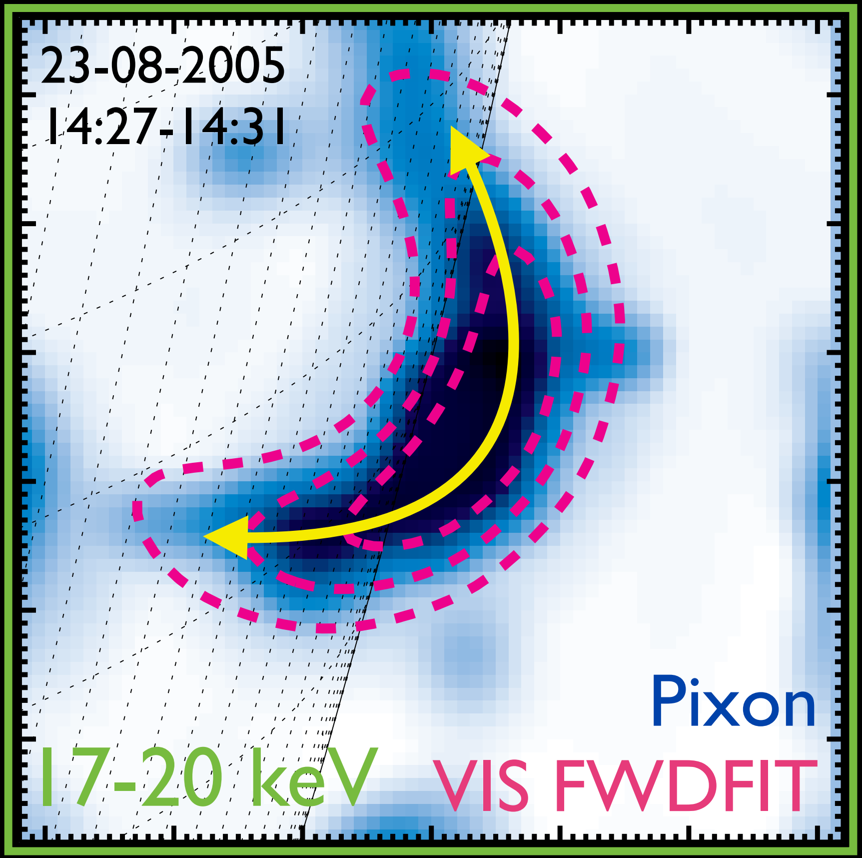

- Each of our chosen events were previously studied by Xu et al. (2008) and Kontar et al. (2011) - i.e. see Iain's talk.
- All three events are similar M-class flares.
- Using different imaging algorithms (Clean and Pixon), each source appears as a loop-like structure that can be fitted with a VIS FWDFIT loop.

Loop length FWHM $\longrightarrow$ measured in the direction parallel to the guiding field.

Finding suitable coronal events

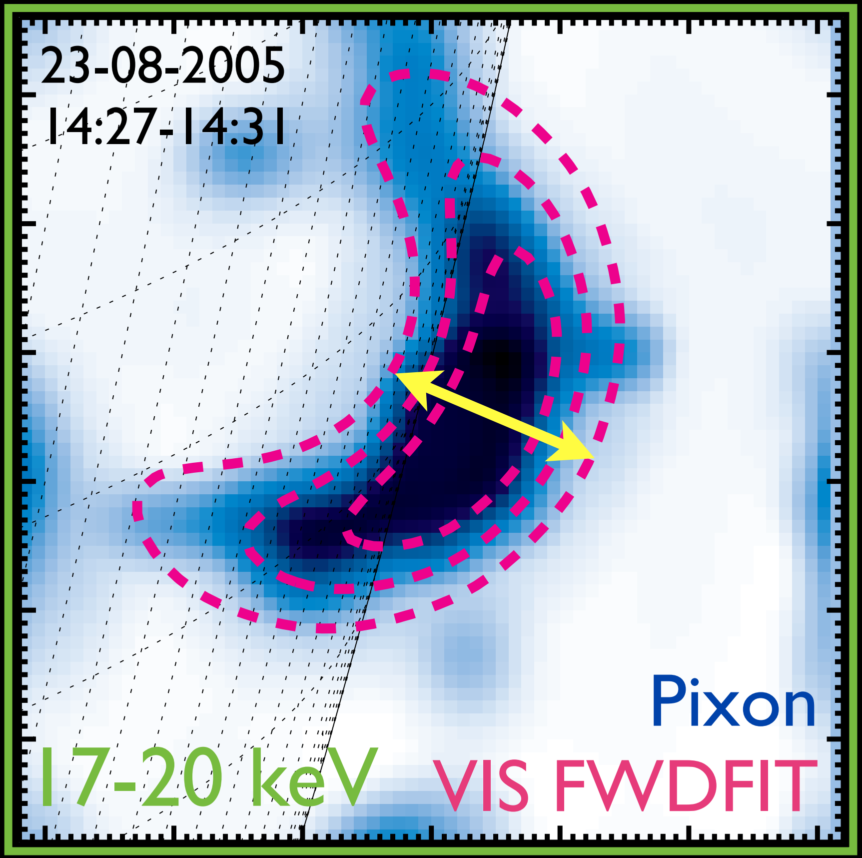

- Each of our chosen events were previously studied by Xu et al. (2008) and Kontar et al. (2011) - i.e. see Iain's talk.
- All three events are similar M-class flares.
- Using different imaging algorithms (Clean and Pixon), each source appears as a loop-like structure that can be fitted with a VIS FWDFIT loop.

Loop length FWHM ⟶ measured in the direction parallel to the guiding field.

Loop width FWHM ⟶ measured in the direction perpendicular to the guiding field.

RHESSI and Visibility forward fitting (VIS FWDFIT)

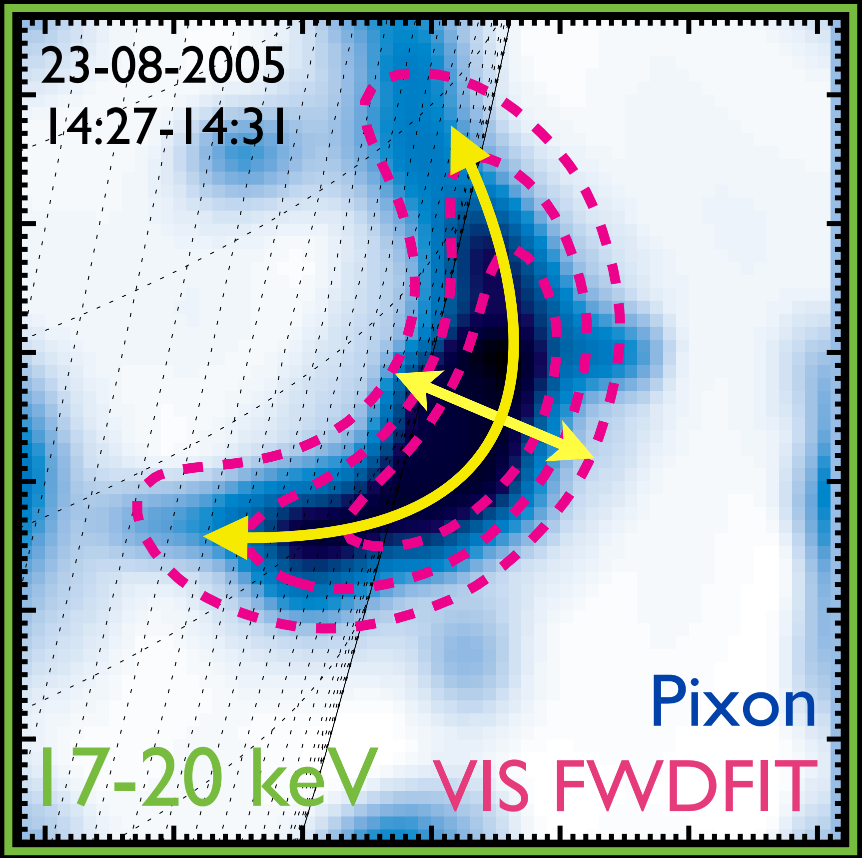

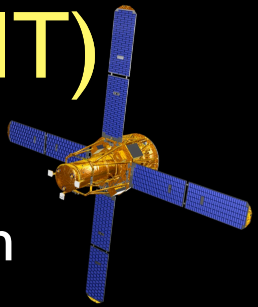

- RHESSI uses rotating modulation collimators, i.e. pairs of grids.
- The spacecraft spins - grids placed in front of the 9 detectors each produce a modulation curve.
- The amplitudes and phases of each modulation curve = X-ray visibilities. These visibilities contain the source spatial information.

VIS FWDFIT takes a chosen known form, such as an elliptical gaussian and compares this with the real X-ray visibilities for a chosen number of detectors.

RHESSI and Visibility forward fitting (VIS FWDFIT)

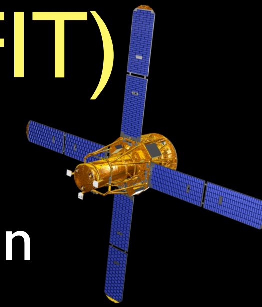

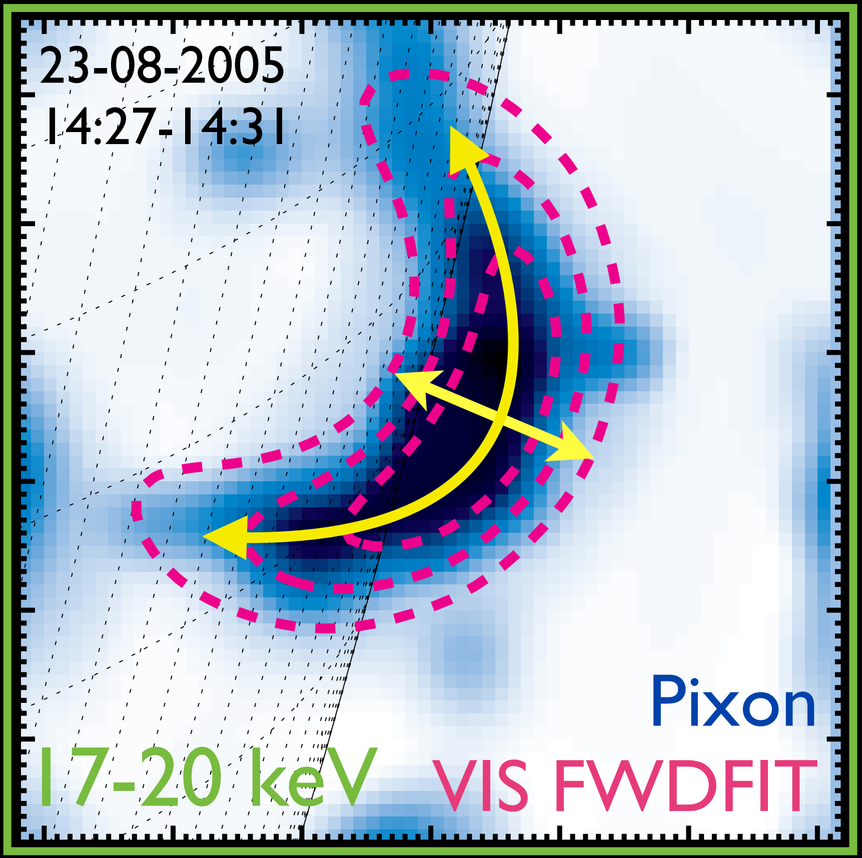

- RHESSI uses rotating modulation collimators, i.e. pairs of grids.
- The spacecraft spins - grids placed in front of the 9 detectors each produce a modulation curve.
- $$V(u, v; \epsilon) = \int_x \int_y I(x, y; \epsilon) e^{2\pi i (xu+yv)} dx dy,$$

VIS FWDFIT takes a chosen known form, such as an elliptical gaussian and compares this with the real X-ray visibilities for a chosen number of detectors.

RHESSI and Visibility forward fitting (VIS FWDFIT)

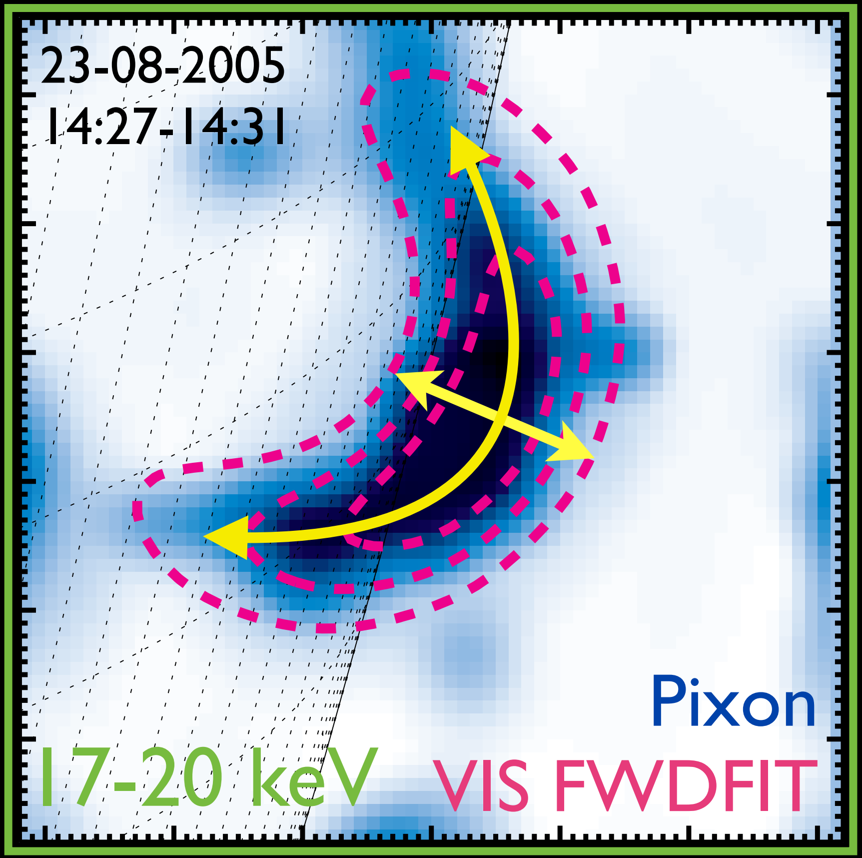

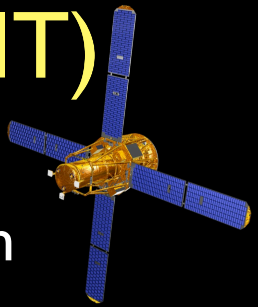

- RHESSI uses rotating modulation collimators, i.e. pairs of grids.
- The spacecraft spins and the grids placed in front of the 9 detectors each produce a modulation curve.
- The amplitudes and phases of each modulation curve = X-ray visibilities. These visibilities contain the source spatial information.

Advantage - For a good fit, VIS FWDFIT gives both the source parameters plus errors, i.e. semi-major axis ± error or x position ± error.

RHESSI and Visibility forward fitting (VIS FWDFIT)

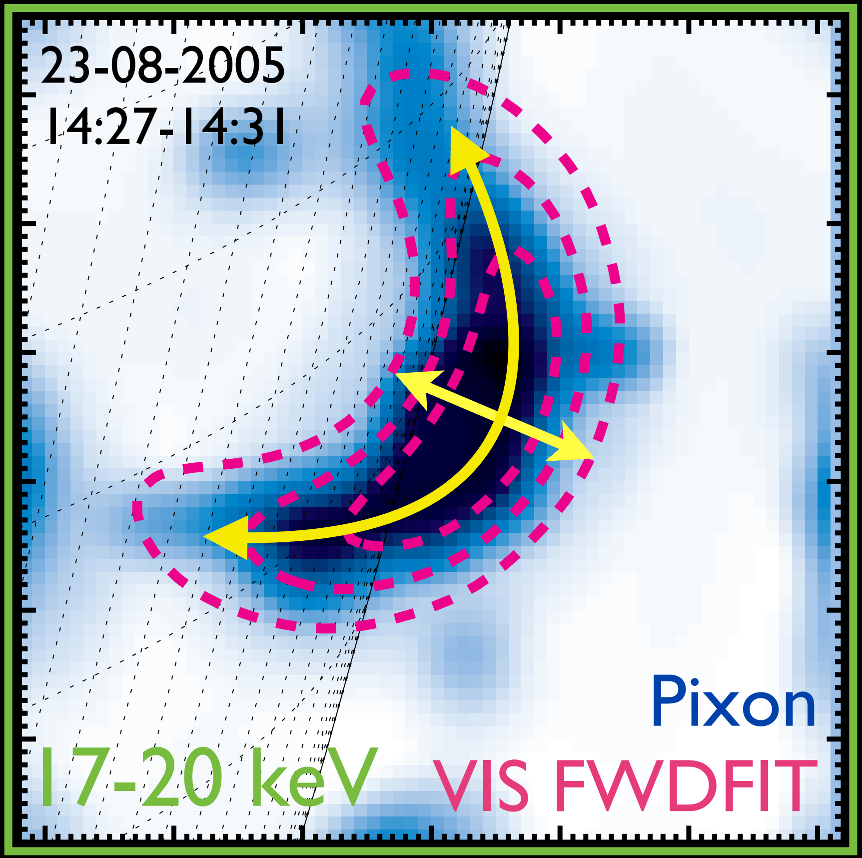

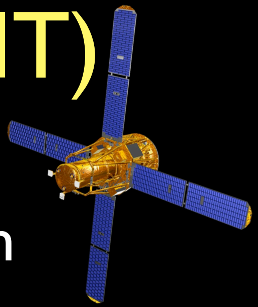

- RHESSI uses rotating modulation collimators, i.e. pairs of grids.
- The spacecraft spins and the grids placed in front of the 9 detectors each produce a modulation curve.
- The amplitudes and phases of each modulation curve = X-ray visibilities. These visibilities contain the source spatial information.

Disadvantage - The shape of source you are fitting has to resemble one of the three chosen forms of circular, elliptical or curved elliptical (i.e. a loop) gaussian.

Chosen events - Imaging

1. 23rd August 2005

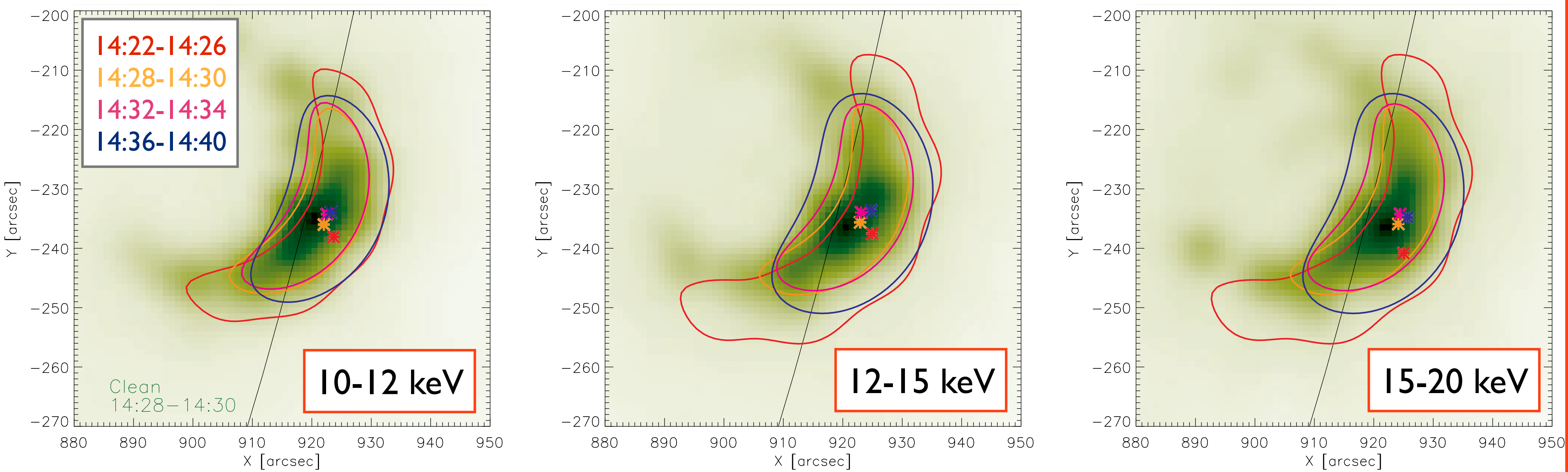

- Limb event with coronal emission in the range ~ 10-25 keV.
- Imaging times - 14:22:00-14:26:00, 14:26:00-14:28:00, 14:28:00-14:30:00, 14:30:00-14:32:00, 14:32:00-14:34:00, 14:34:00-14:36:00 and 14:36:00-14:40:00.
- Spatially large event with 30-40 keV footpoints emerging at ~ [880, −240] and [893, −200] at ~14:36:00.

Chosen events - Imaging

2. 14th/15th April 2002

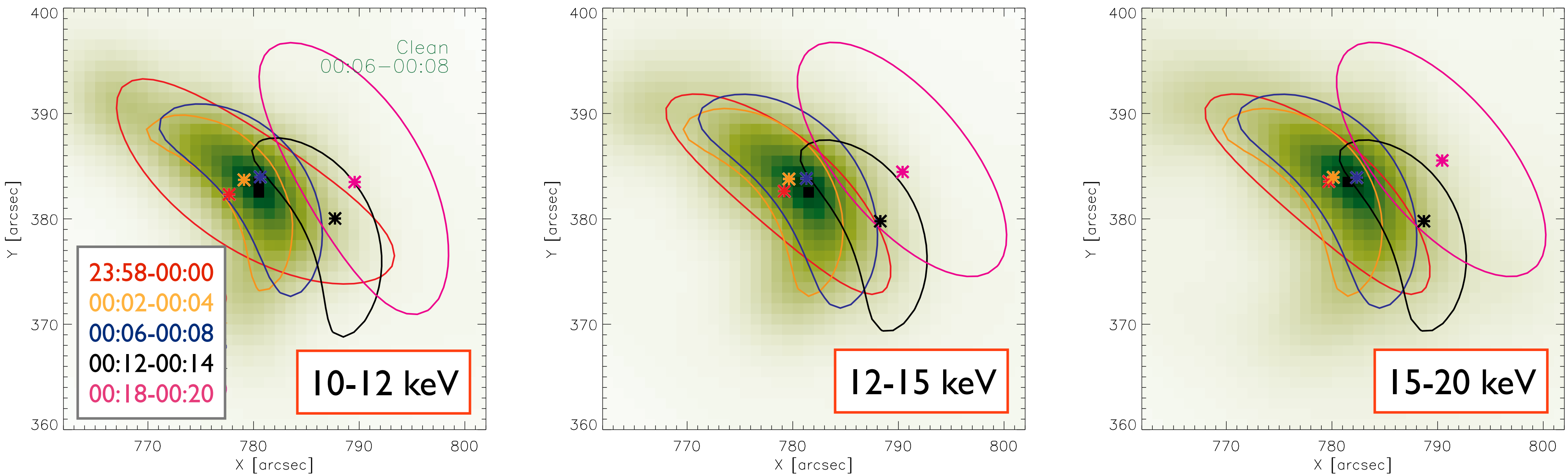

- Disk event with coronal emission in the range ~ 10-25 keV.
- Imaging times - two minute intervals from 23:58:00 to 00:20:00.
- Appearance of two 30-40 keV footpoints at ~[760,390] and [774,369].

Chosen events - Imaging

3. 21st May 2004

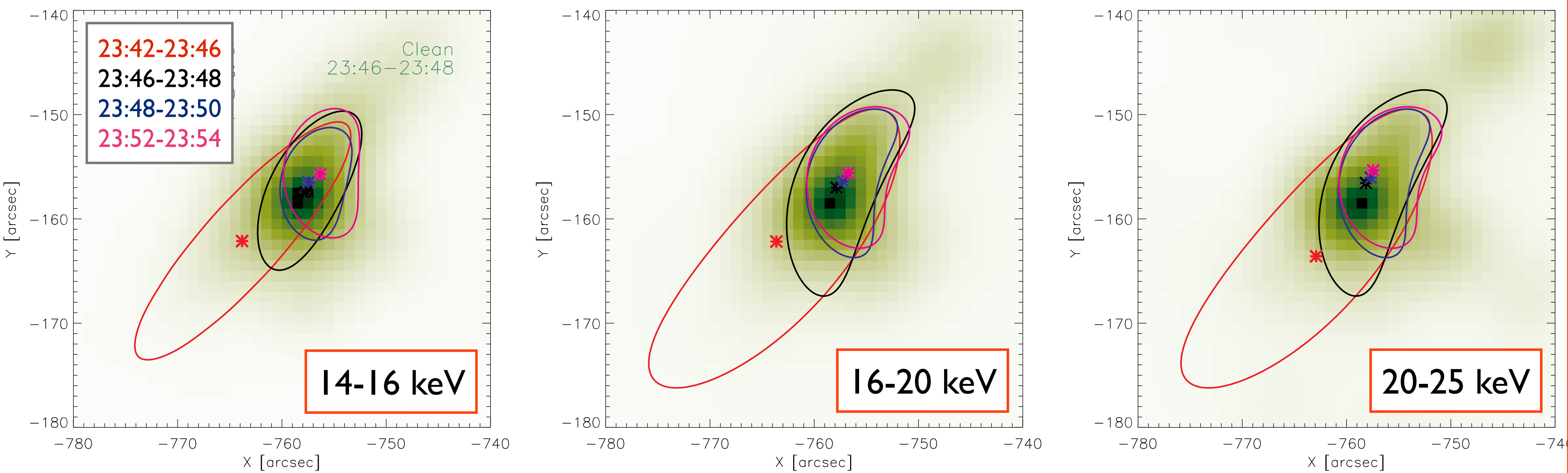

- Disk event with coronal emission in the range ~ 10-25 keV.
- Imaging times - 23:42:00-23:46:00, 23:46:00-23:48:00, 23:48:00-23:50:00, 23:50:00-23:52:00, 23:52:00-23:54:00 and 23:54:00-23:58:00.
- Weak footpoint emission at all ~times at ~ [-745,-165] and [-745,-140].

Loop VIS FWDFIT parameters

1. 23rd August 2005

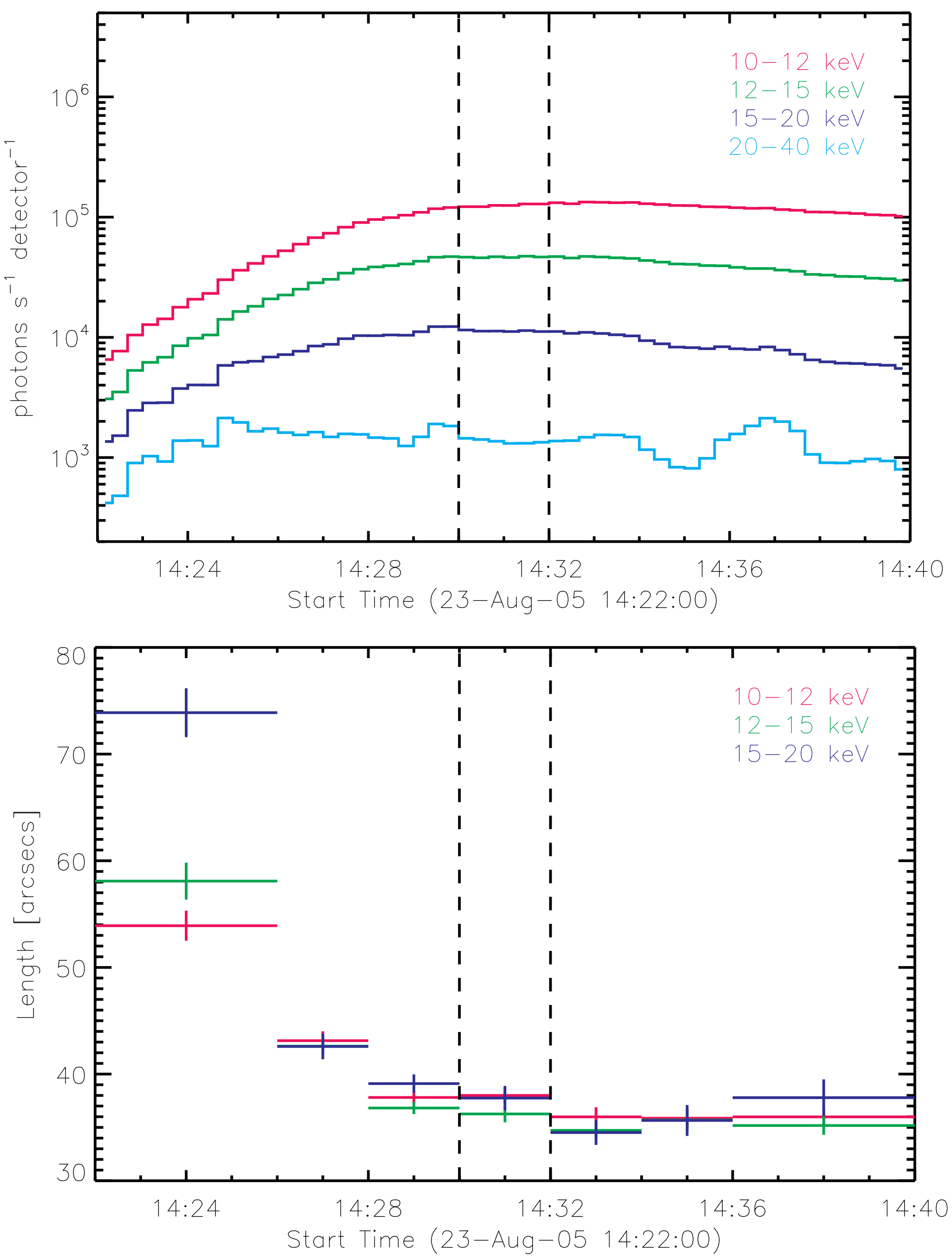

Length changes with time

- steep decline in loop length before the ~ peak in X-ray emission.

- steeper decline for higher energy ranges.

- loop length remains ~ constant/slight increase after the peak in X-ray emission.

Loop VIS FWDFIT parameters

1. 23rd August 2005

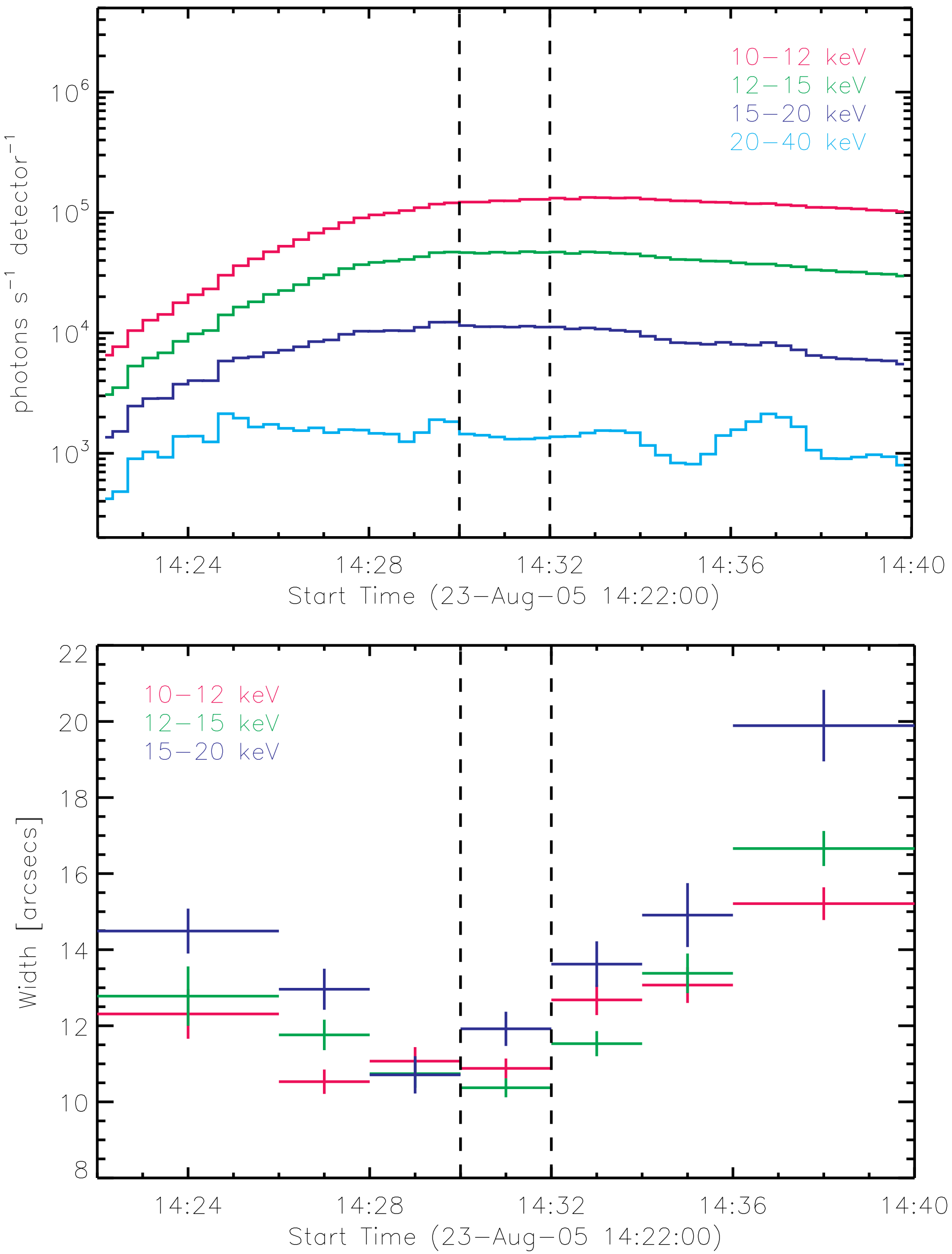

Width changes with time

- decrease in loop width before ~ peak in X-ray emission.

- increase in loop width after ~ peak in X-ray emission.

- Expands faster after peak than contraction before peak.

Loop VIS FWDFIT parameters

1. 23rd August 2005

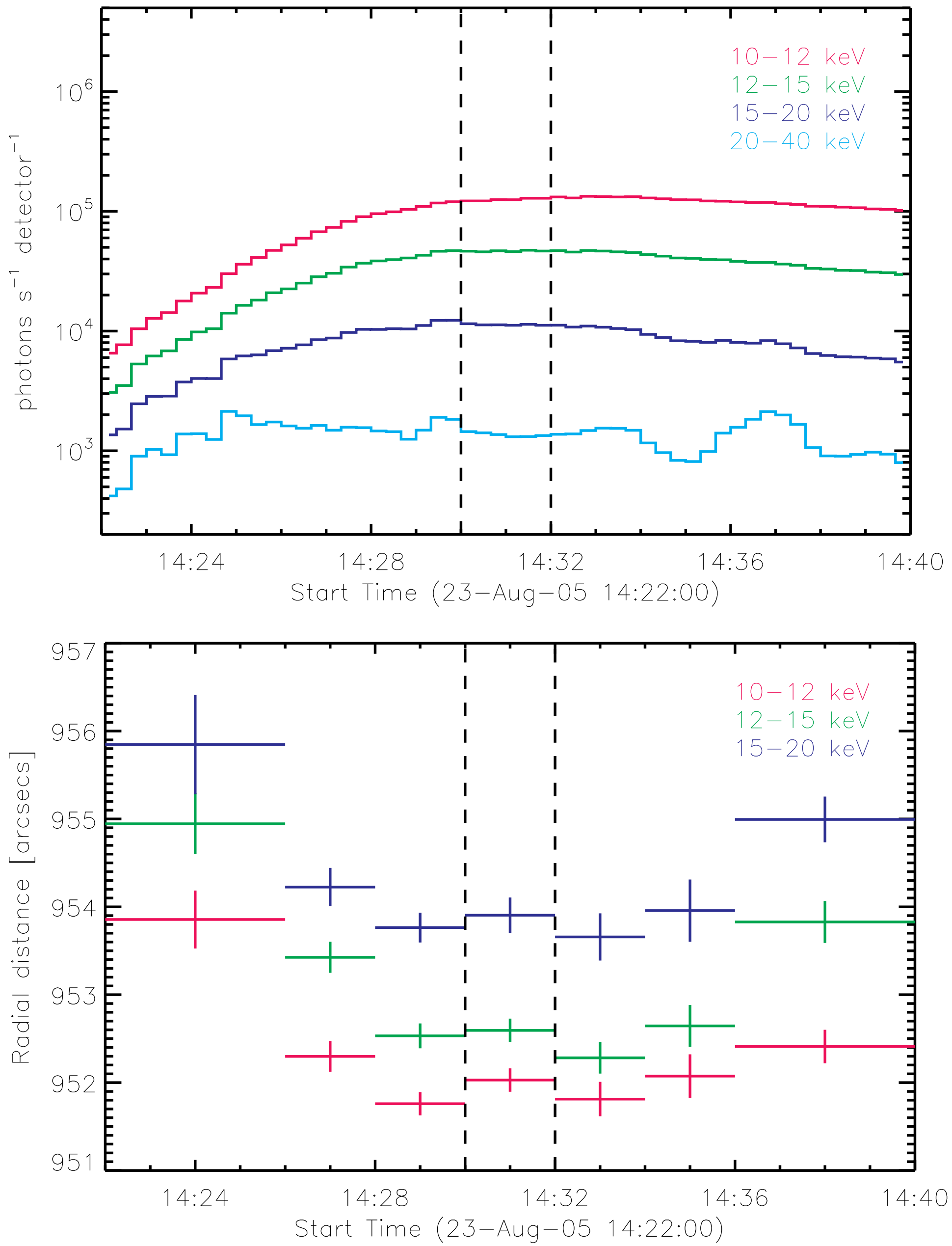

Position changes with time

- radial distance/altitude decreases before ~ peak in X-ray emission.

- radial distance/altitude increases after the ~peak in X-ray emission.

- ~ same increase/decrease rate for all three energies plotted.

Spectroscopy parameters

1. 23rd August 2005

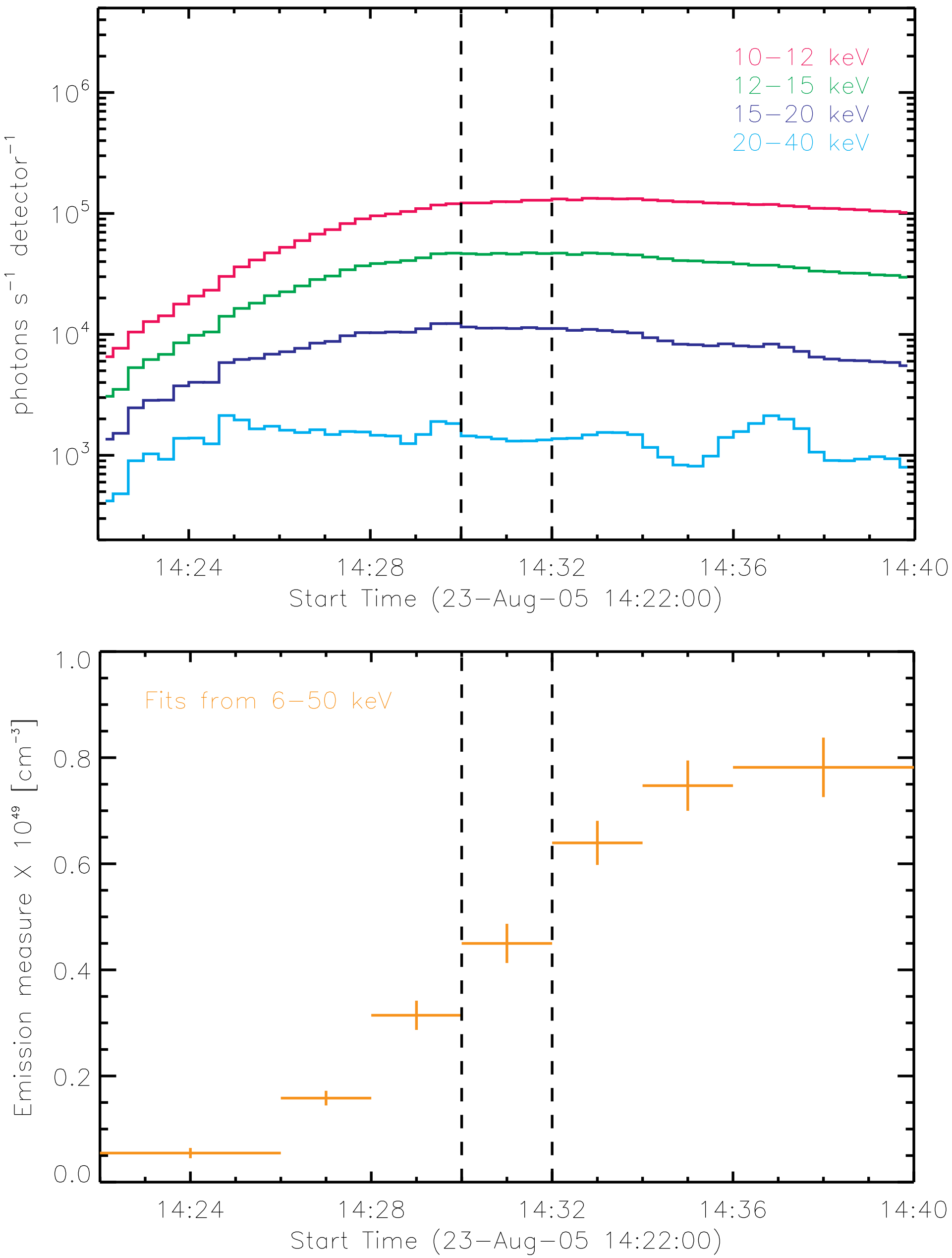

Spectroscopy was performed for each imaging interval at 6-50 keV.

Thermal + thick target bremsstrahlung fits.

The thermal part gives us the emission measure and plasma temperature.

1. Emission measure, EM:

- The EM increases during the imaging time interval.

Spectroscopy parameters

1. 23rd August 2005

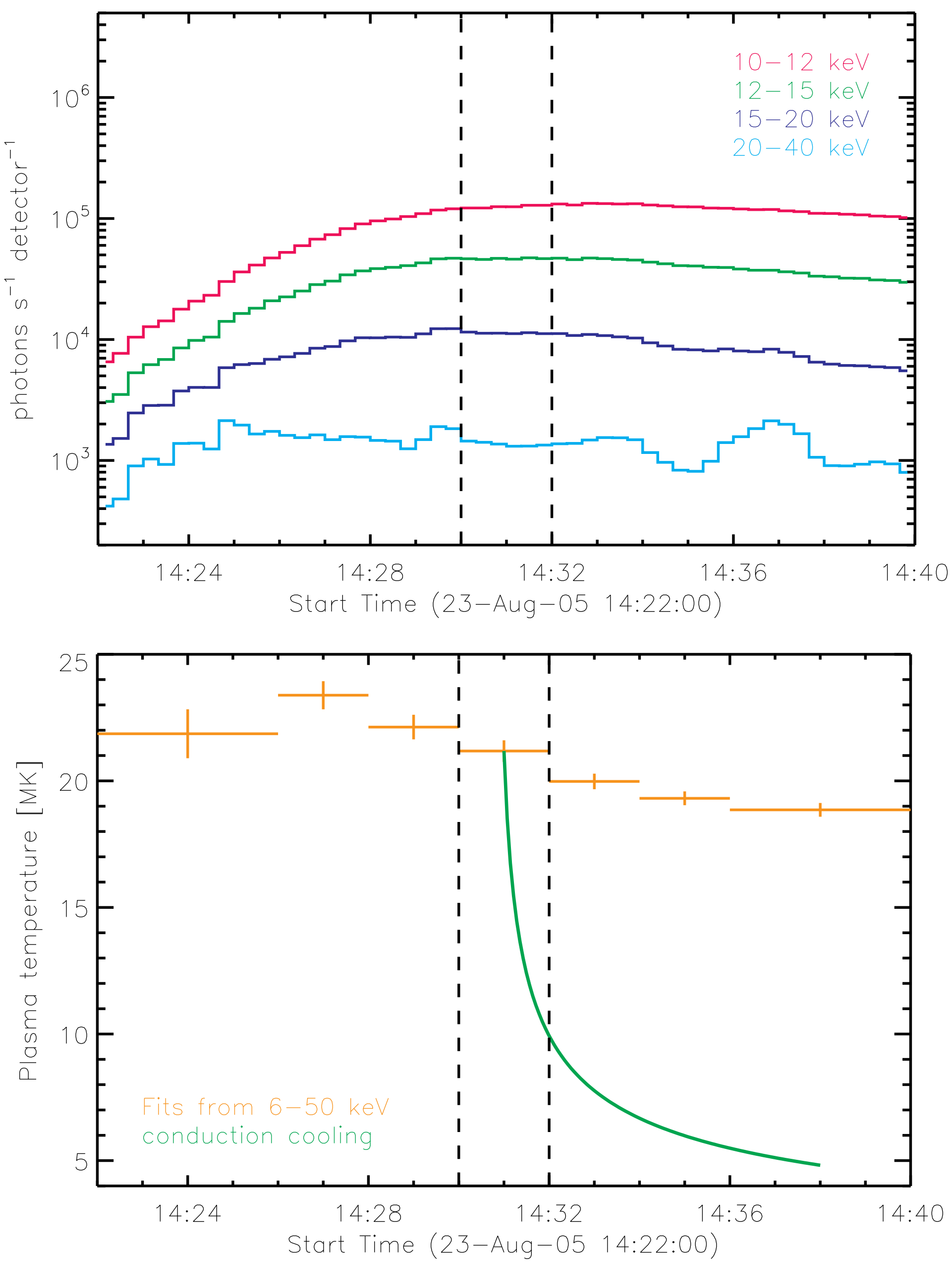

Spectroscopy was performed for each imaging interval at 6-50 keV.

Thermal + thick target bremsstrahlung fits.

The thermal part gives us the emission measure and plasma temperature.

2. Plasma temperature, T:

- Apart from the first time interval, T decreases during the imaging time interval.

Spectroscopy parameters

1. 23rd August 2005

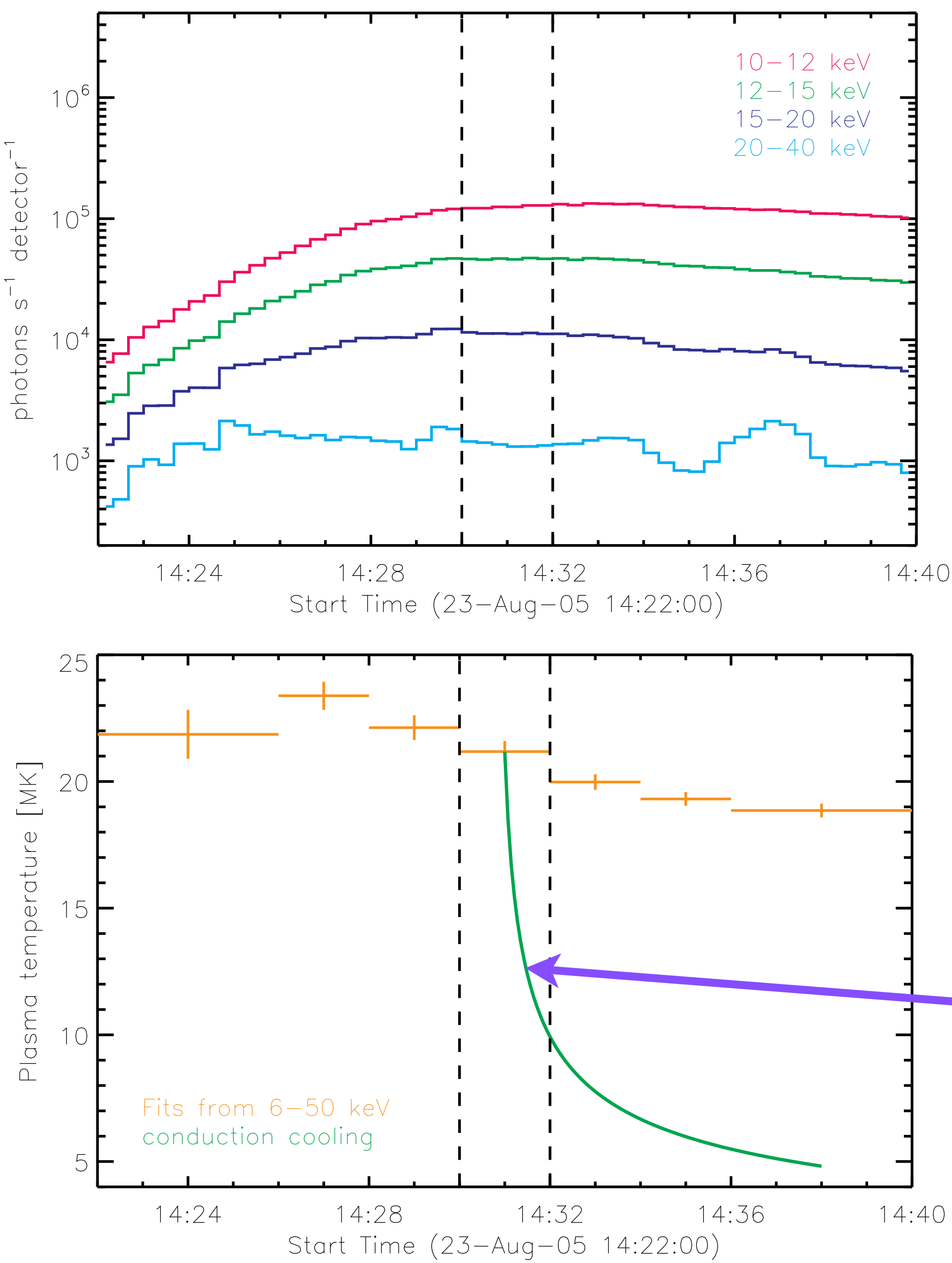

Spectroscopy was performed for each imaging interval at 6-50 keV.

Thermal + thick target bremsstrahlung fits.

The thermal part gives us the emission measure and plasma temperature.

2. Plasma temperature, T:

- Comparison with conduction cooling only where $T = (T_p^{-5/2} + Ct)^{-2/5}$, where $C \sim 2 \times 10^{10}\, n^{-1}\, L^{-2}$. (Culhane et al. (1970))

Other inferred parameters

1. 23rd August 2005

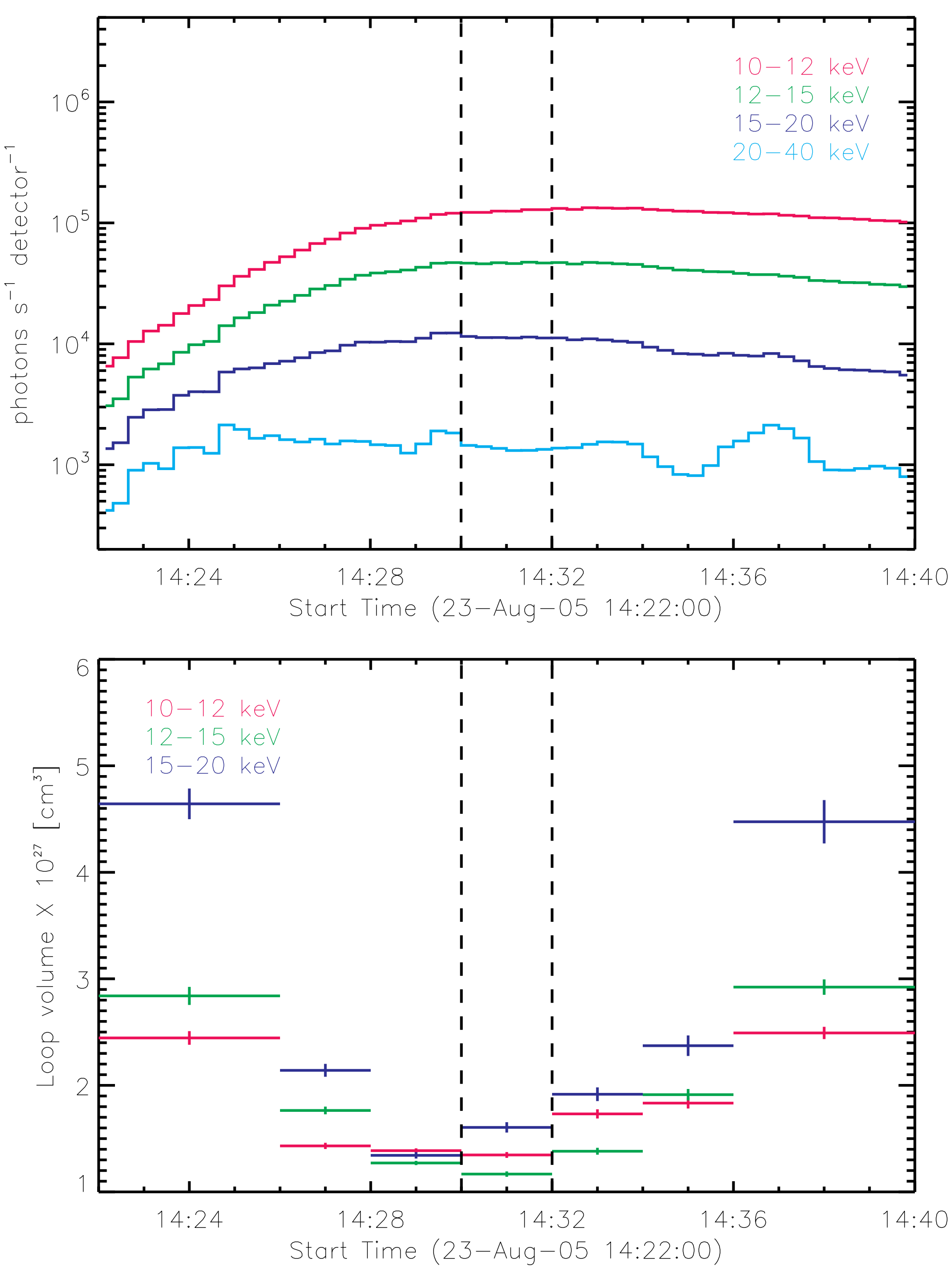

From imaging and spectroscopy we can infer:

1. Loop volume

The loop volume is measured as,

$$\boxed{V = \frac{\pi W^2 L}{4}}$$

with width W and length L.

As expected from L and W, the loop volume decreases before the ~ peak in X-ray emission and increases after this time.

Other inferred parameters

1. 23rd August 2005

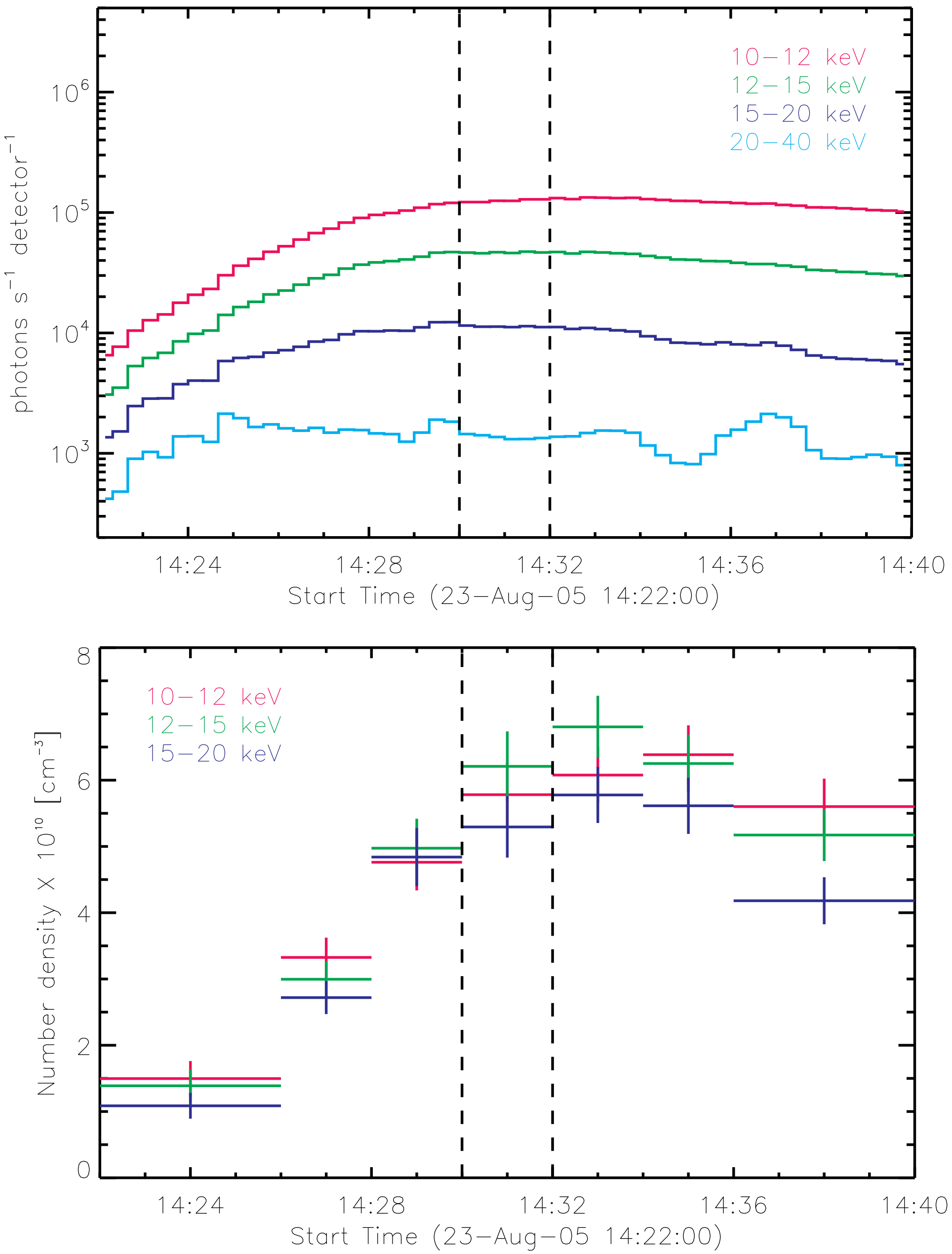

From imaging and spectroscopy we can infer:

2. Number density

From the loop volume and EM we can work out the number density using,

$$\boxed{n = \sqrt{EM/V}}$$

Number density increases until around 14:33:00 (just after the peak) and then starts to decreases again.

Other inferred parameters

1. 23rd August 2005

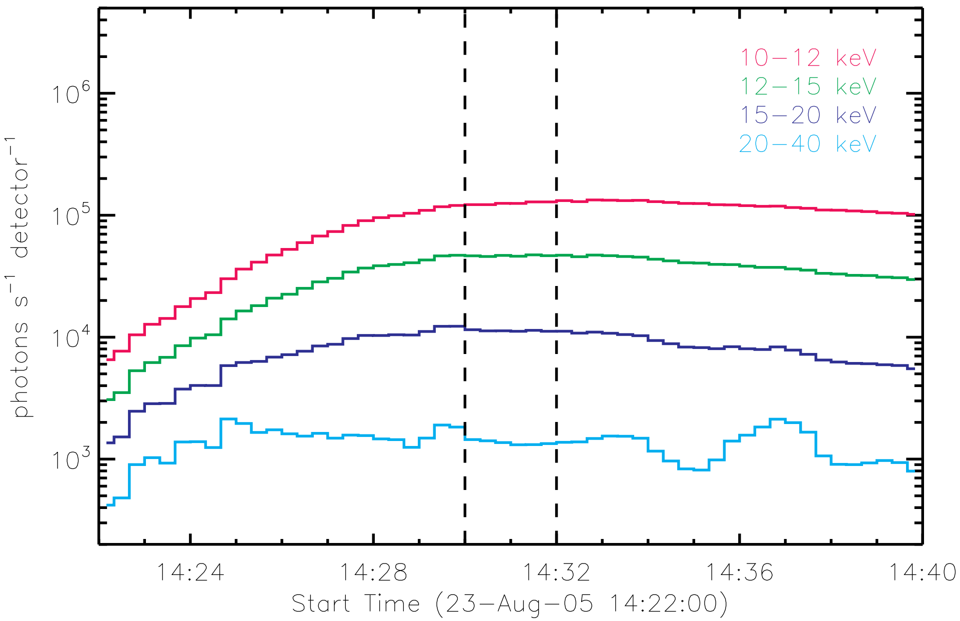

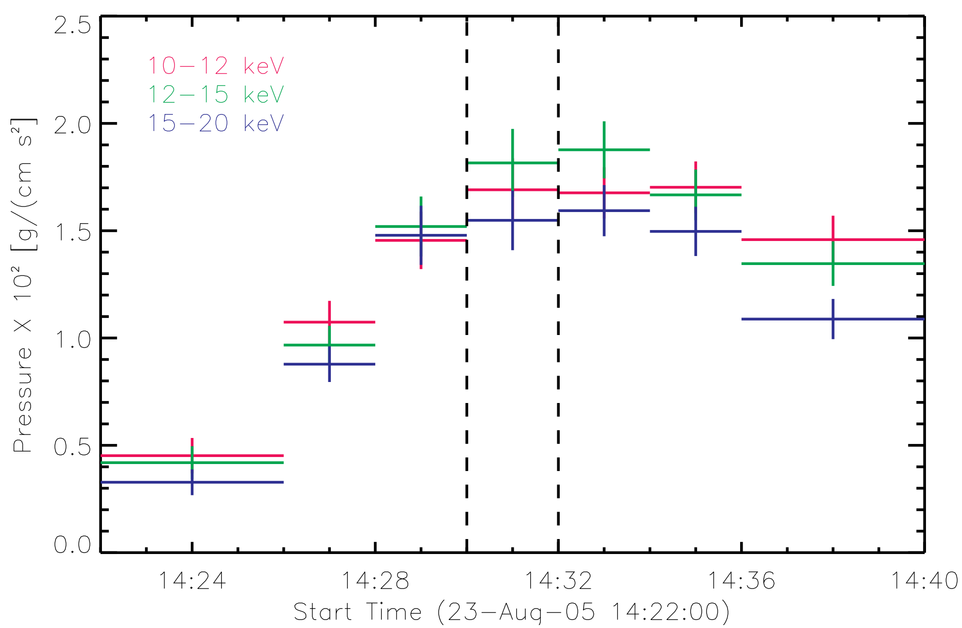

From imaging and spectroscopy we can infer:

3. Pressure

From the number density and plasma temperature we can work out the pressure using,

$$\boxed{P = nk_BT}$$

Pressure increases until 14:33:00, just after the peak X-ray emission and then starts to decrease after this time.

Other inferred parameters

1. 23rd August 2005

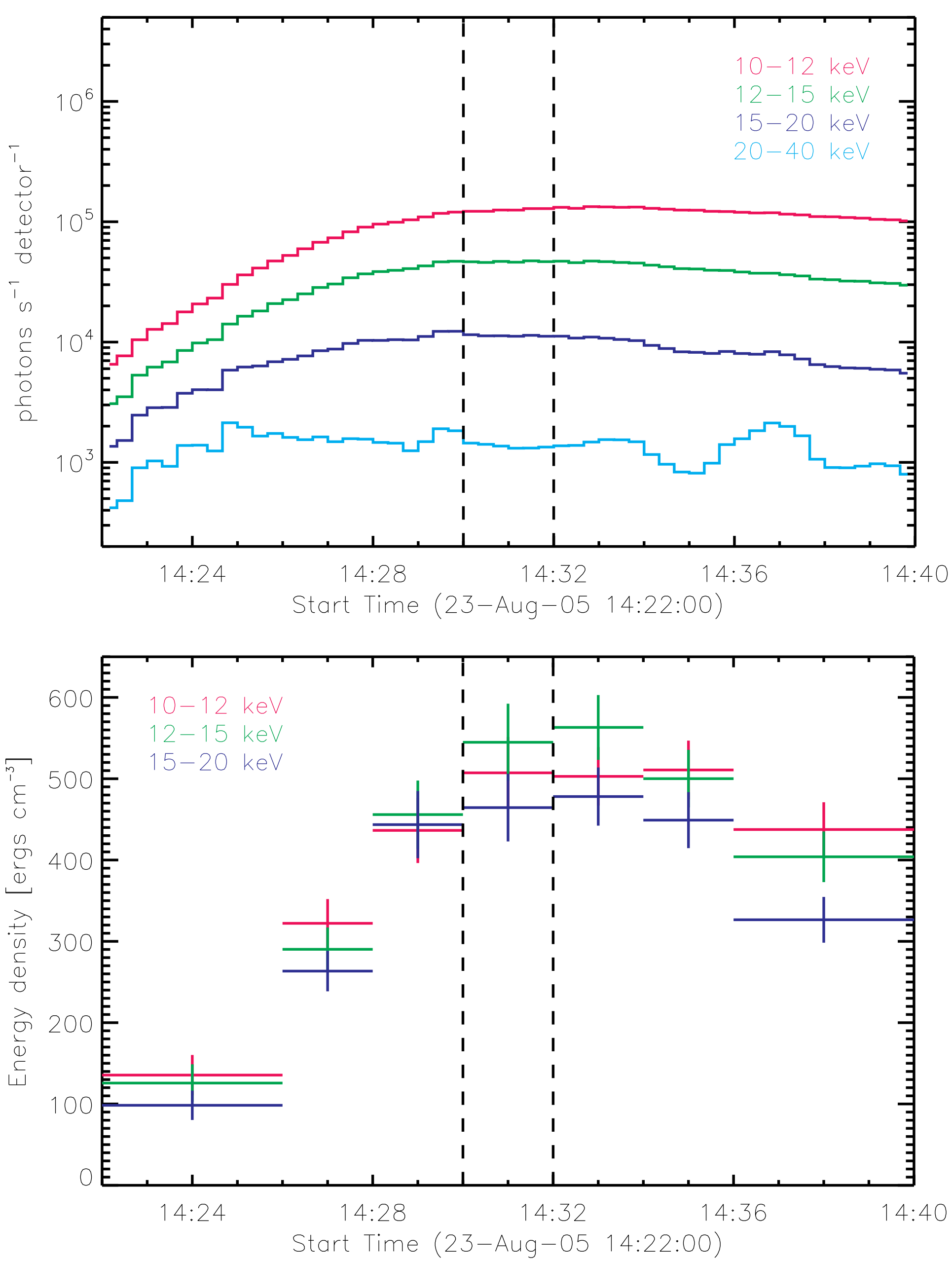

From imaging and spectroscopy we can infer:

4. Energy density

The number density and plasma temperature also give us the energy density,

$$\boxed{E = 3nk_BT}$$

Follows the same pattern as the pressure multiplied by 3, with the peak ~ coinciding with the peak in X-ray emission.

Comparison of results for all 3 events

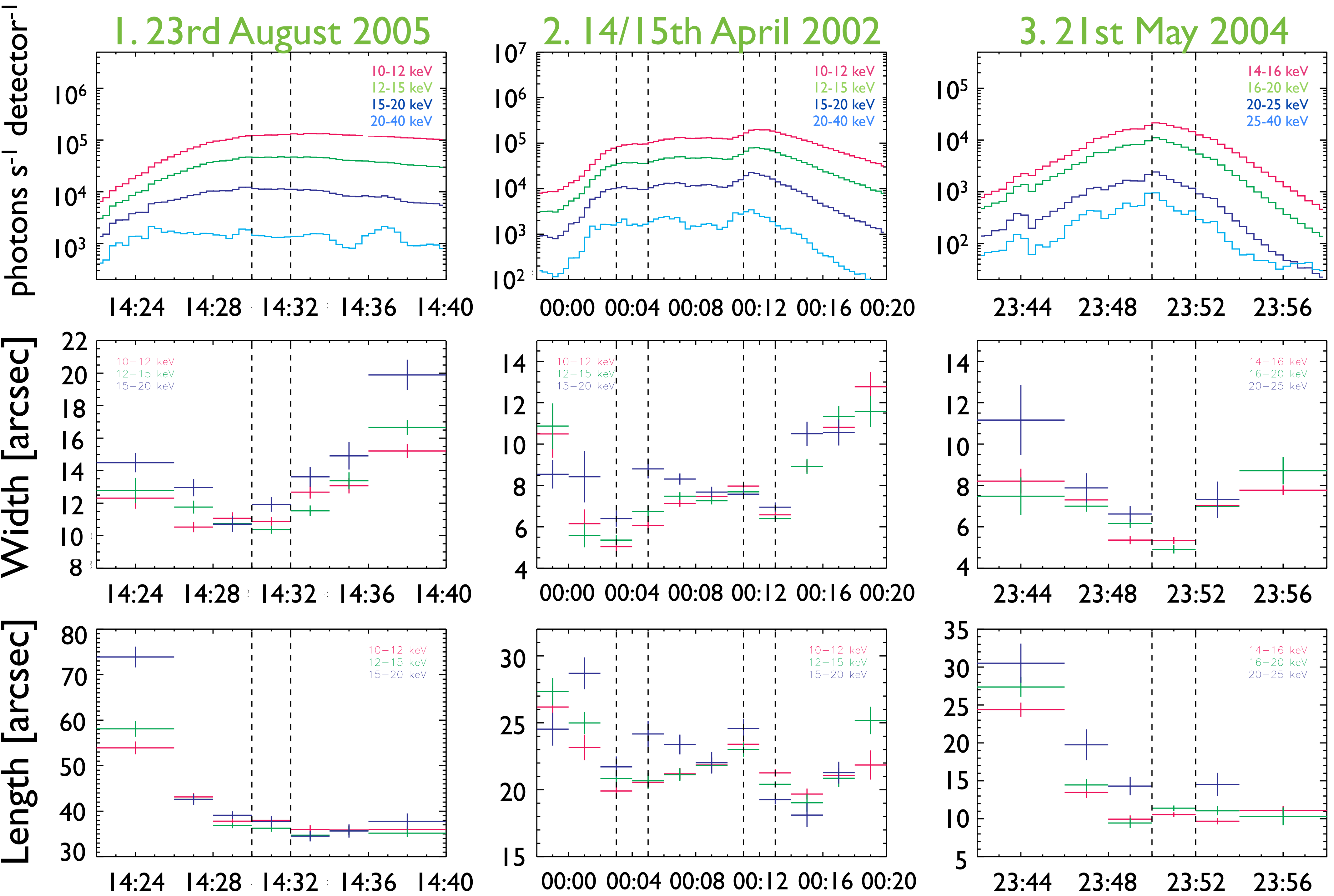

Comparison of results for all 3 events

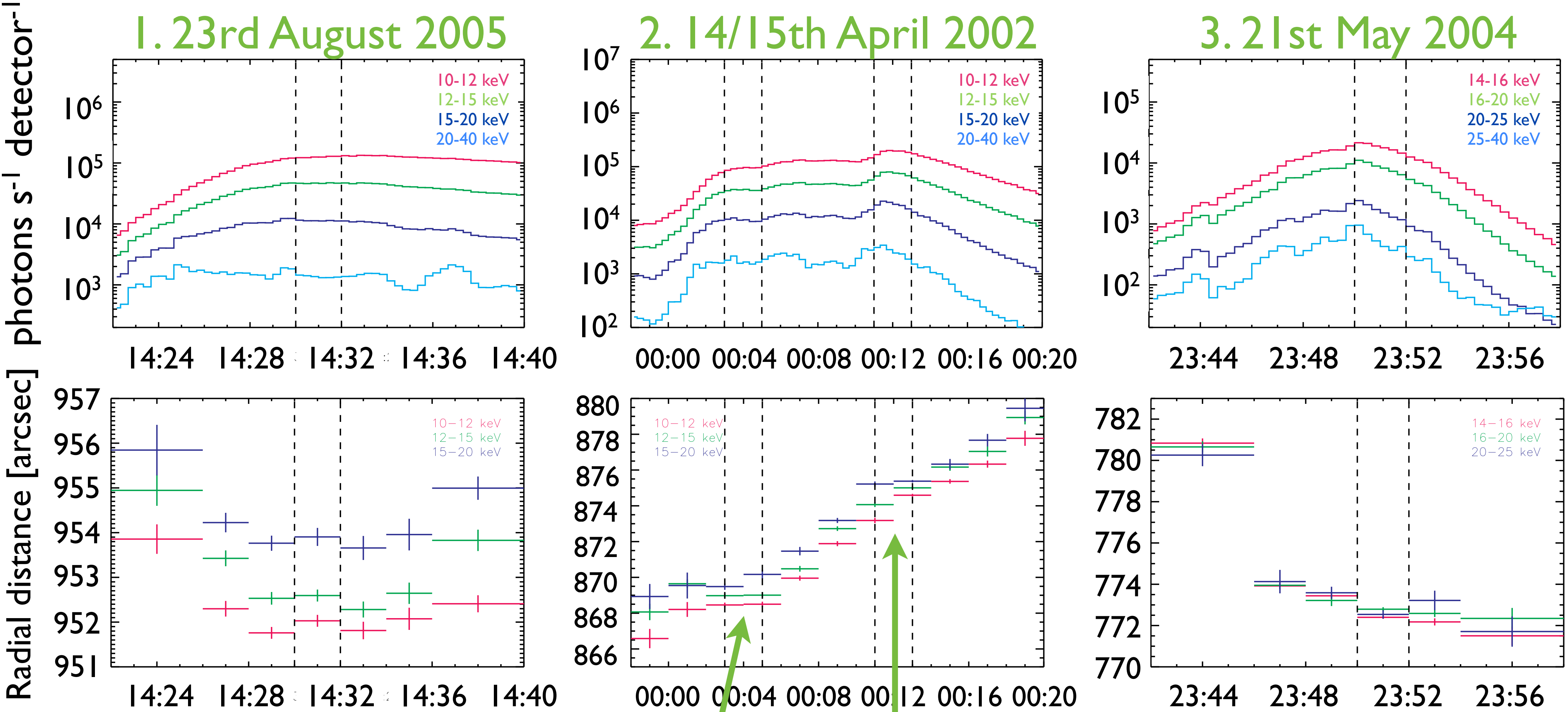

Hard to say whether an altitude decrease or increase occurs for the disk events - we can only say a changes occurs at each peak!

Comparison of results for all 3 events

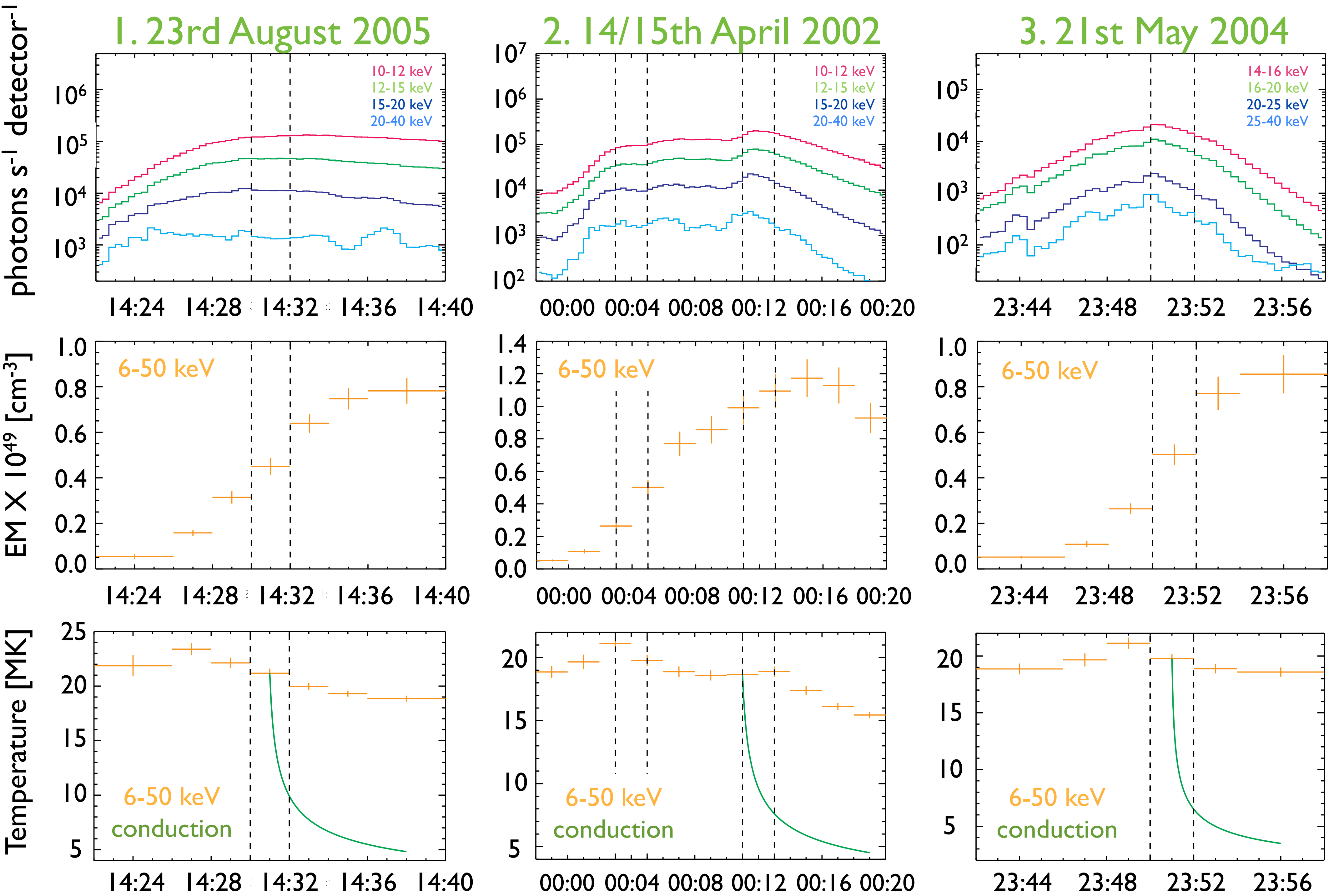

Comparison of results for all 3 events

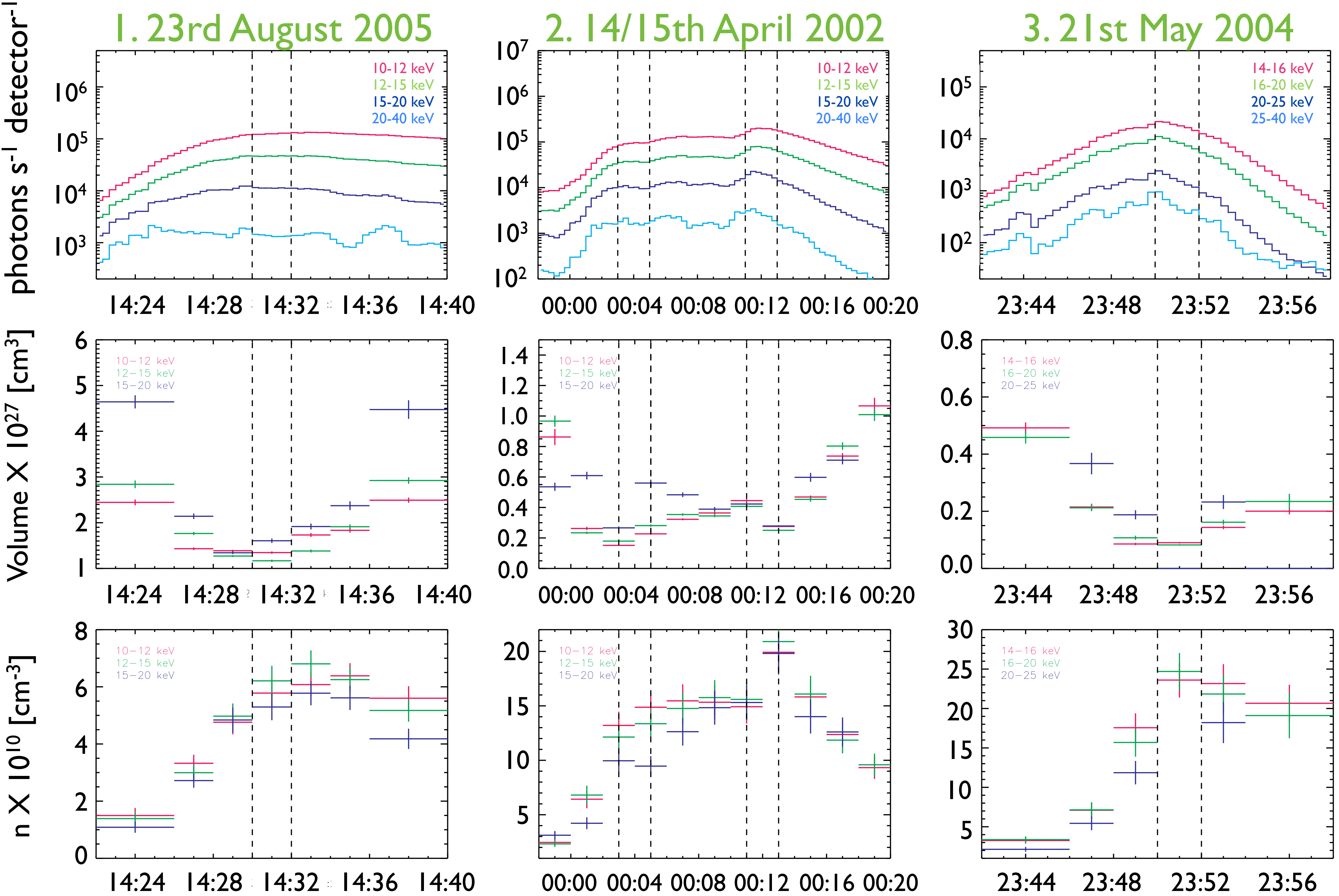

Comparison of results for all 3 events

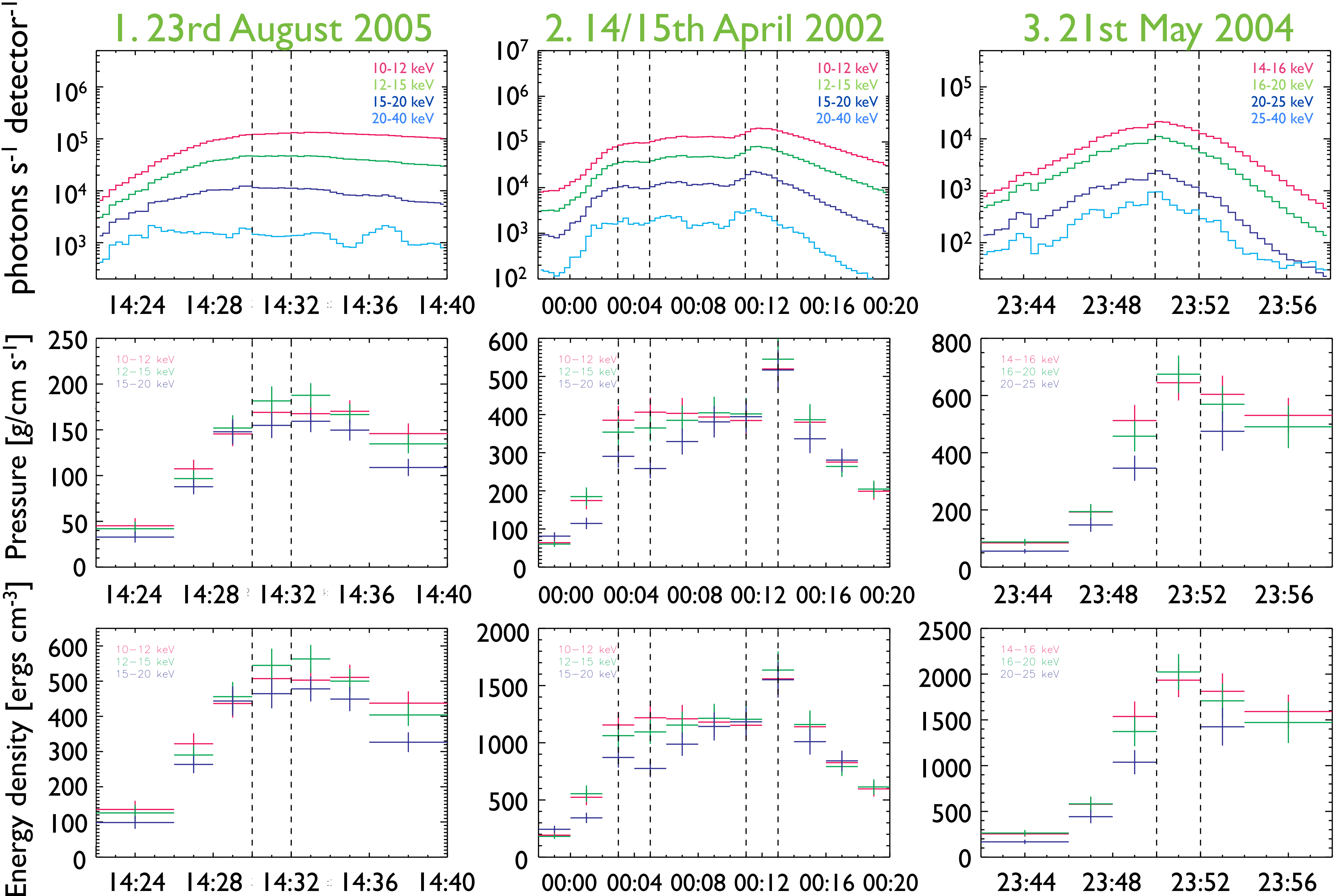

Results summary

All three events showed similar changes in their spatial and spectral properties.

- Loop size contracts while the X-ray emission increases, with increases in number density, pressure and energy density.

For flare 1 (10-12 keV), $\Delta L \sim 14''$, $\Delta W \sim 2''$ and $\Delta R \sim 2''$.

For flare 2 (10-12 keV), $\Delta L \sim 7''$, $\Delta W \sim 6''$ and $\Delta R \sim 2''$.

For flare 3 (10-12 keV), $\Delta L \sim 5''$, $\Delta W \sim 2''$ and $\Delta R \sim 2''$.

Contraction of loop size > changes in loop position.

Results summary

All three events showed similar changes in their spatial and spectral properties.

- Loop size expands after the peak X-ray emission, with decreases in number density, pressure and energy density.

For flare 1 (10-12 keV), $\Delta L \sim 1''$, $\Delta W \sim 4''$ and $\Delta R \sim 0.5''$.

For flare 2 (10-12 keV), $\Delta L \sim 2''$, $\Delta W \sim 7''$ and $\Delta R \sim 3''$.

For flare 3 (10-12 keV), $\Delta L \sim 1''$, $\Delta W \sim 3''$ and $\Delta R \sim 1''$.

Expansion of loop size (esp. width) > changes in loop position.

Results summary

To our knowledge, this is the first time that the loop size compression and expansion has been measured during the flare duration.

But,

Many people have noted the height contraction/expansion before/after the peak of the impulsive phase: Sui & Holman (2003); Sui et al. (2004); Veronig et al. (2006) and Joshi et al. (2009), Lui et al. (2009) and Gosain et al. (2012) etc.

↓ ↓ ↓ ↓ ↓ ↓ ↓

Collapsing magnetic trap??

Magnetic field relaxes to a state of lower energy during reconnection (Taylor (1974)) → field lines need to contract in some way?

After impulsive peak, chromospheric evaporation drives expansion?

Previous results involving coronal implosion

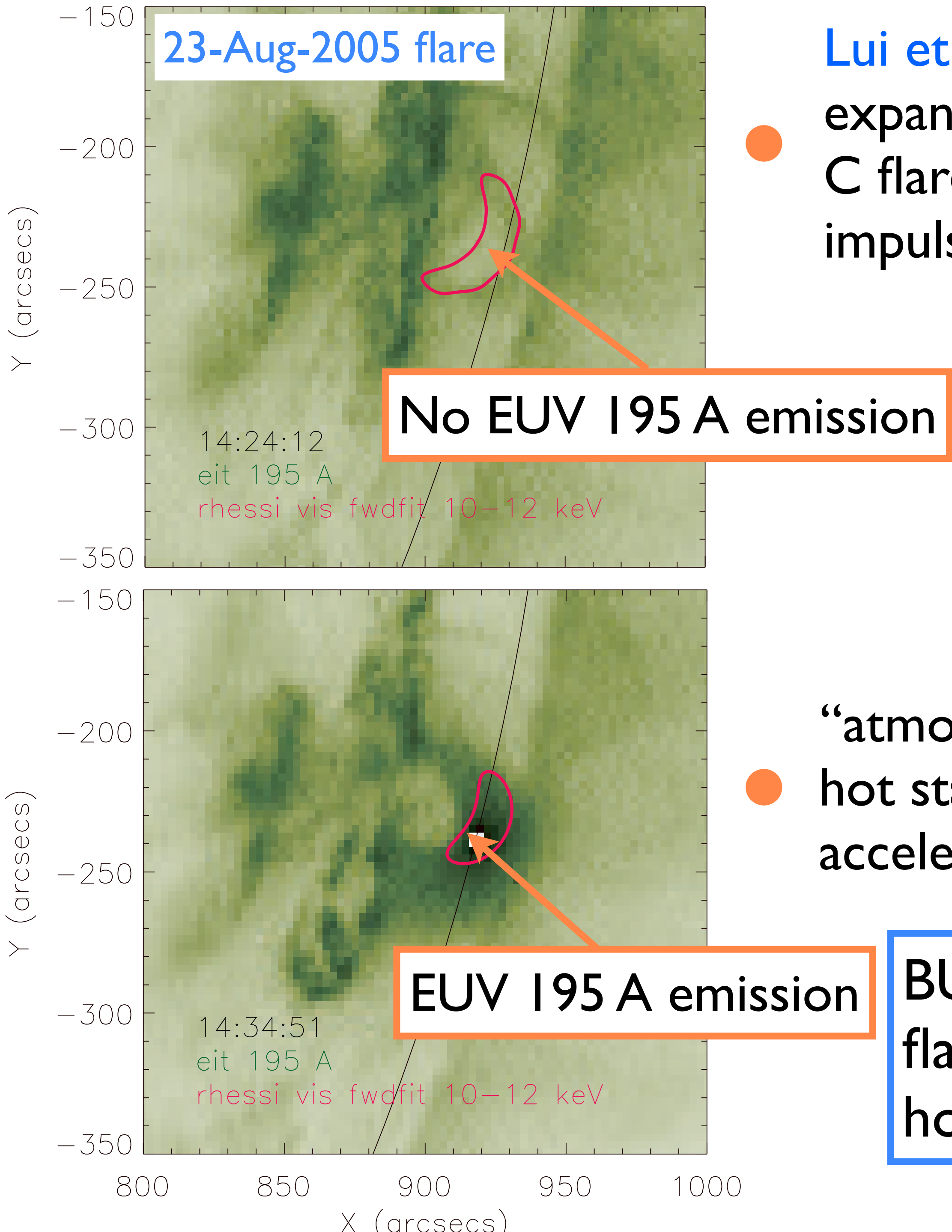

- Lui et al. (2009) noted the contraction/expansion (altitude increase/decrease) of a C flare in EUV and X-ray before/after the impulsive peak.
  - Energy conversion process
    → Reduction in B pressure
    → Loop contraction (height)
    (loop size compression also?)
- "atmosphere already heated to a dense and hot state prior to impulsive electron acceleration."

BUT from EIT images of 23-08-2005 flare, no EUV but X-ray emission = hot, dense plasma.